# Chapter 9
# Experimental Observation of Polarization Bremsstrahlung on Atoms, Clusters and Solids

## 9.1 Bremsstrahling on Atoms with Account for the Polarization Channel

### *9.1.1 Early Investigations*

One of the first experiments for PBs on atoms was the work of the E.T. Verkhovtseva's group [1], studied in which was the contribution of the "atomic" component of Bs to the spectrum of bremsstrahlung of electrons with the energy 600 eV scattered by xenon gas in a photon energy range of 70–150 eV. In this spectral range a "giant resonance" takes place in the xenon photoabsorption $\sigma_{ph}(\omega)$, the said resonance being caused by the 4d-subshell of an atom, which according to the optical theorem

$$\mathrm{Im}\{\alpha(\omega)\} = \frac{c}{4\pi\omega}\,\sigma_{ph}(\omega) \tag{9.1}$$

is indicative of the high value of the imaginary part and, as a consequence, of the squared absolute value of the atomic polarizability $|\alpha(\omega)|^2$ that defines the contribution of the polarization channel to the total Bs. The last statement follows, for example, from the formula (3.24).

It should be noted that in early investigations of PBs several terms for designation of the polarization channel in bremsstrahlung were used in literature: polarization Bs, atomic Bs, dynamic Bs, parametric X-radiation, and transient Bs in plasma (see Chap. 1). For example, in the cited paper the polarization Bs channel was called the atomic channel.

Given in Fig. 9.1a from the paper [1] is the comparison of the intensity of polarization Bs on a xenon atom measured in a spectral range of 70–150 eV with PBs calculated by the formula analogous to Eq. 3.29. In Fig. 9.1b the dynamic polarizability of a xenon atom in a corresponding region of photon energies is presented. The squared absolute value of the dynamic polarizability included in

V. Astapenko, *Polarization Bremsstrahlung on Atoms, Plasmas, Nanostructures and Solids*, Springer Series on Atomic, Optical, and Plasma Physics 72,
DOI 10.1007/978-3-642-34082-6_9, © Springer-Verlag Berlin Heidelberg 2013

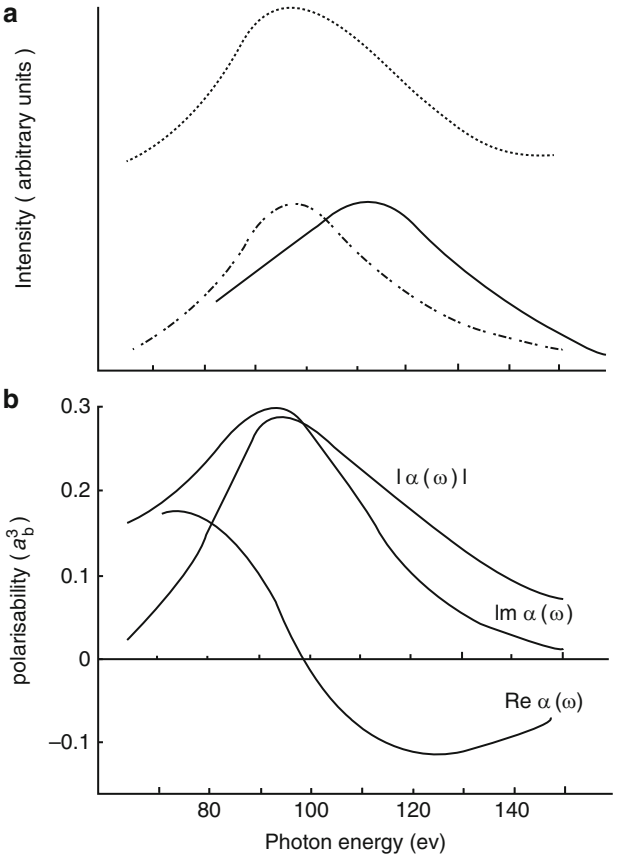


**Fig. 9.1** (**a**) The comparison of the measured spectrum of atomic (polarization) Bs of an electron on a xenon atom (*solid curve*) with the calculated PBs spectrum (*dash-and-dot curve*), the photoabsorption spectrum is represented by a *dashed curve*; (**b**) the magnitude, the real and imaginary parts of the dynamic polarizability of a xenon atom calculated by the experimental value of the photoabsorption cross-section [1]

the expression for the PBs cross-section (Eq. 3.29) was calculated with the use of the optical theorem (Eq. 9.1) and the Kramers-Kronig relation for the real part of the polarizability

$$\mathrm{Re}\alpha(\omega) = \frac{1}{\pi}\,\mathrm{V.P.}\int_0^\infty \frac{\mathrm{Im}\alpha(\omega')}{\omega'^2 - \omega^2}\,d\omega'^2 \tag{9.2}$$

by the cross-section of photoabsorption $\sigma_{ph}(\omega)$ taken from the experimental work [2].

It should be noted that the electron energy was limited to the value 600 eV to avoid ionization of the 3d-subshell of xenon and resulting radiation at the transition

$4p^5 4d^9 \rightarrow 4p^6 4d^8$ in the spectral range under study. The concentration of particles in the interaction zone was $(5 \div 8) \times 10^{15}$ cm$^{-3}$, so the absorption of Bs on xenon atoms did not exceed 5 % in this frequency region.

To determine the atomic contribution to the process, from the spectrum of Bs of electrons on xenon the spectrum of Bs on argon was subtracted. This method is justified by the fact that PBs on argon in the spectral range under consideration is negligible.

From Fig. 9.1 the correlation of the measured PBs spectrum and the frequency dependence of the magnitude of the dynamic polarizability of a xenon atom in the spectral range under consideration is seen. In this case the maximum of the PBs spectrum fell on a photon energy of 113 eV, which considerably exceeds the energy of ionization of the 4d-subshell of xenon. The FWHM of the measured spectrum was 47 eV. The PBs intensity at the maximum of the frequency dependence was 70 % of the intensity of ordinary (electron) Bs according to the theoretical estimate made in the work [3].

PBs in the considered case is formed as a result of virtual excitation of xenon electrons to an ionization continuum above the threshold of ionization of the 4d-subshell. The authors of the work [1] connected the distinction between the obtained experimental data and the theoretical PBs spectrum (the dash-and-dot curve in Fig. 9.1) with a relatively low value of electron beam energy (600 eV) for validity of the PBs theory based on the Born approximation.

In the work [3] published a year before the paper [1], radiation of electrons with the energy of 500 eV scattered by metal lanthanum in a photon energy range of 100–140 eV was measured. In this frequency region the photoabsorption of metal lanthanum is close to atomic, which gave the authors of the cited paper reason to believe that the radiation spectrum is also of an atomic nature. A satisfactory agreement of the measured spectrum with the calculation based on the theory of PBs of fast electrons was found out.

The results of further experimental investigations of PBs of electrons on xenon atoms carried out by E.T. Verkhovtseva with co-authors are presented in the paper [4]. In this work the spectrum of radiation arising in electron scattering by xenon atoms in a photon energy range of 80–220 eV was measured. The energy of an electron beam varied within 300–900 eV.

In the cited work it was found that the position of the spectral maximum of radiation $\omega_{max}$ depends on the energy of scattered electrons and the radiation angle (between the electron velocity and the wave vector of a photon). This dependence is connected with the large width of the spectral maximum of radiation $\Gamma$ that is in turn caused by a giant resonance in the spectrum of photoabsorption of a xenon atom in the spectral range under consideration (Fig. 9.2a).

In the Born-Bethe approximation, in the paper [4] the following expression for the shift of the PBs maximum with respect to the maximum of the frequency dependence of the squared absolute value of the dynamic polarizability of an atom $\omega_0$ for a radiation angle of 90° was derived:

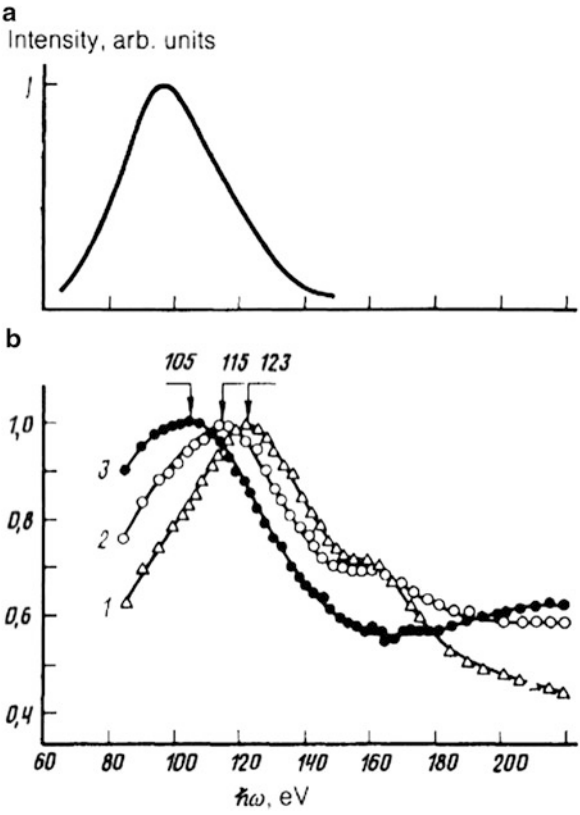


**Fig. 9.2** (**a**) The spectrum of photoabsorption of a xenon atom; (**b**) Bs of electrons scattered by a xenon atom with different energies: *curve 1* – 300 eV, *curve 2* – 600 eV, *curve 3* – 900 eV. All spectra are normalized to their values at the maximum [4]

$$\omega_{\max} - \omega_0 \simeq \frac{2\,\Gamma^2}{\omega_0}\,\frac{1 + 5\,\varepsilon L/4}{1 + \left[1 - 5\,(\Gamma/\omega_0)^2/2\right]\varepsilon L}, \tag{9.3}$$

where $\varepsilon = m\hbar\,\omega/p^2$ ($p$ is the initial electron momentum, $\hbar\,\omega$ is the energy of a bremsstrahlung photon), $L = \ln\left(\gamma\,\frac{\mathrm{v}^2}{\omega^2 R_a^2}\right)$ is the Coulomb logarithm (v is the initial electron velocity, $R_a$ is the mean atomic radius, $\gamma$ is the factor of the order of one). In the limit $\varepsilon \to 0$ the formula (9.3) for the frequency of the Bs spectrum maximum gives: $\omega_{\max} \to \omega_0 + 2\,\Gamma^2/\omega_0$. Thus even in the limit of high electron energies there is a shift of the Bs spectrum maximum with respect to the spectral maximum of the magnitude of the dynamic polarizability of an atom. From the obtained limiting relation it follows also that the spectral shift under consideration is noticeable if the ratio of the parameters $\Gamma/\omega_0$ is great enough.

Since ordinary (electron) Bs is a smooth function of the photon frequency and the radiation angle, the shift of the spectral maximum is caused mainly by the polarization channel.

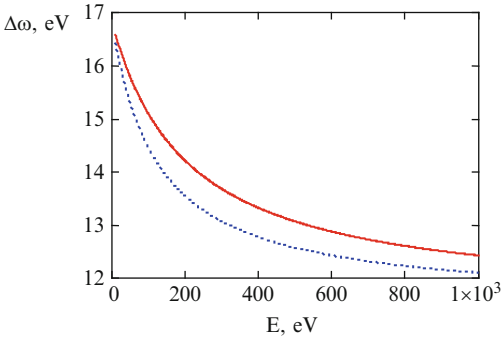


**Fig. 9.3** The dependence of the shift of the spectral maximum of PBs in a photon energy range of 100–140 eV on the energy of an electron scattered by a xenon atom, for two values of the Coulomb logarithm: *solid curve* – L (the Coulomb logarithm) = 10, *dotted curve* – L = 6; the radiation angle 90°

From the Eq. 9.3 it follows that the shift of the spectral maximum of PBs for a radiation angle of 90° is always positive and decreases with growing electron energy. Both these facts are in conformity with the experimental data obtained in the work [4] (see Fig. 9.2b).

The plot of the function (Eq. 9.3) (depending on the electron energy) is presented in Fig. 9.3 for two values of the Coulomb logarithm and the following values of parameters: $\hbar\omega_0 = 100$ eV, $\hbar\Gamma = 24$ eV.

The comparison with experimental data shows that the theoretical shift of the frequency of the spectral maximum of PBs decreases with growing electron energy more slowly than it was observed in the work [4], which is apparently explained by insufficiency of the Born-Bethe approximation for quantitative description of Bs of electrons with a specified energy.

So experimentally demonstrated in the cited paper was the importance of taking into account the polarization channel in consideration of Bs on atom in the frequency range where the dynamic polarizability of an atom is high.

### *9.1.2 Measurements of the Absolute Value of the Cross-Section of Bs of Fast Electrons on Atoms*

The measurements of the absolute double-differential Bs cross-section (depending on the frequency and the angle of photon emission) in scattering of electrons with an energy of 28 and 50 keV on atoms of noble gases were for the first time carried out in the work [5] in a wide spectral range from 5 keV to the kinematic limit, the radiation angle was 90°.

The results of experiments were compared with calculations of the cross-section of ordinary Bs and total Bs (in view of the polarization channel). Corresponding plots are presented in Figs. 9.4 and 9.5 [5].

The calculation of total Bs was carried out in the so-called “atom stripping” approximation (stripping approximation) [6]. The main idea of this approximation is that the PBs amplitude and the screening summand in the amplitude of ordinary

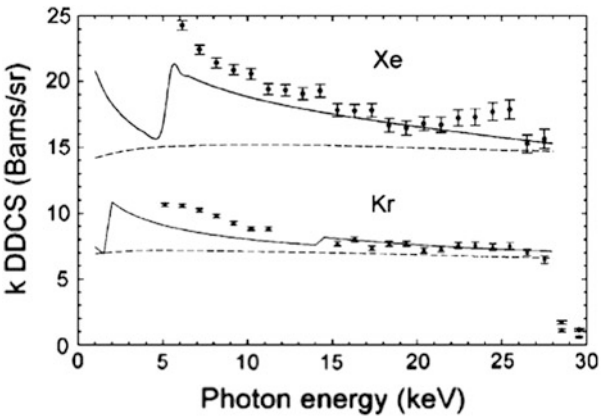


**Fig. 9.4** The measured and calculated cross-sections of Bs of an electron with an energy of 28 keV scattered by krypton and xenon atoms [5]: *solid curves* – the calculated cross-section of total Bs in the stripping approximation; *dashed curves* – the calculated cross-section of ordinary Bs, *black circles* – the experiment [5]

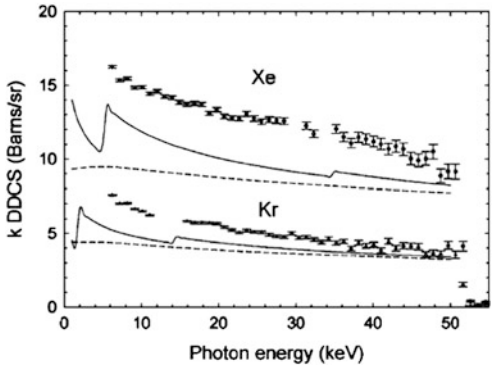


**Fig. 9.5** The same as in Fig. 9.4 for an electron energy of 50 keV [5]

Bs on an atom cancel out [7], and the Bs process in the zeroth approximation proceeds as on a "bare" nucleus.

The cross-section of ordinary Bs was calculated in the relativistic approximation of partial waves, corresponding data are given in the work [8].

From the given figures it is seen that the measured cross-section exceeds considerably the calculated data, which to the greatest extent shows itself for a xenon atom, electron energy of 50 keV and in the low-frequency range. The exception is the case of a neon atom (Fig. 9.6) having a low value of dynamic polarizability, as a result, the measured contribution of PBs to the total cross-section of the process is negligible (practically is not visible in the range of an experimental error).

From the given plots it is seen that the experimental value of the total Bs cross-section, as a rule, exceeds its calculated value in the stripping approximation, which is most probably indicative of insufficiency of this approximation in the case under consideration.

As stated by the authors of the paper [5], the results of their work are strongly indicative of the essentiality of the polarization channel contribution to Bs of fast electrons on free atoms (with a considerable dynamic polarizability) in a wide spectral range.

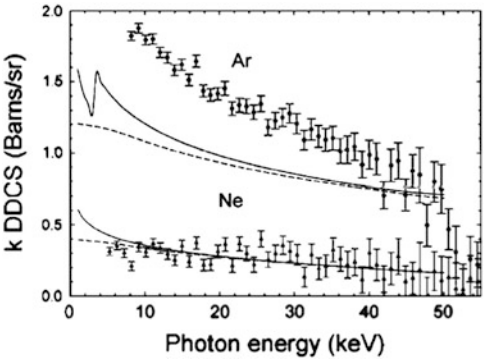


**Fig. 9.6** The same as in Fig. 9.4 for Ar and Ne atoms and an electron energy of 50 keV [5]

### *9.1.3 PBs on Atomic Clusters*

Theoretically the role of cooperative effects in Bs on atomic clusters in a wide spectral range was studied in the author's work [9] by the example of copper clusters (see the Sect. 8.1 of this monograph). In particular, it was shown that cooperative effects are of a considerable importance in PBs of relativistic electrons.

The experimental investigation of Bs of electrons with the energy of 700 eV on xenon atoms and clusters was carried out in the work [10], in which the influence of an ambient medium on the PBs spectrum was taken into account.

Under experimental conditions of [10] a cluster on the average consisted of 20 atoms, and the number of clusters in the volume of interaction was less than 2 % of the total number of particles. In case of changing experimental conditions the number of atoms in a cluster increased from several tens to 8,500.

The results of measurements and calculations of the cited paper are presented in Figs. 9.7 and 9.8.

Corresponding to Fig. 9.7 is a concentration of xenon atoms of $10^{15}$ atoms/cm$^3$. The average number of atoms in a cluster corresponding to Fig. 9.8 is 8,500.

From comparison of the plots of Figs. 9.7 and 9.8 it is seen that in case of clusters the maximum of the PBs spectrum is shifted by 10 eV towards lower photon energies and has a FWHM lesser than for PBs on individual atoms. In both cases the spectral maximum is of an asymmetric form.

The analysis of experimental data carried out in the paper [10] has shown that the reduction of the width of the spectral maximum of PBs with growing number of atoms in a cluster ($N$) at first is slow up to values $N \approx 200$–$300$. Then (for $N > 500$) the sharp reduction of the width of the maximum begins, and the width goes to saturation when the number of atoms in a cluster is several thousands. In this case the width of spectral maximum decreases approximately by 30 %.

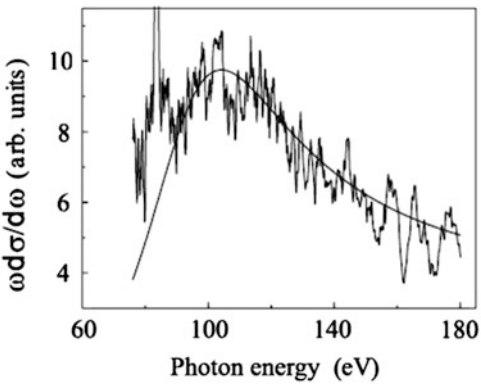


**Fig. 9.7** The spectrum of PBs of an electron with the energy of 0.7 keV on a xenon atom: *"noisy" curve* – experiment, *smooth curve* – calculation in view of the dielectric permittivity of an ambient medium

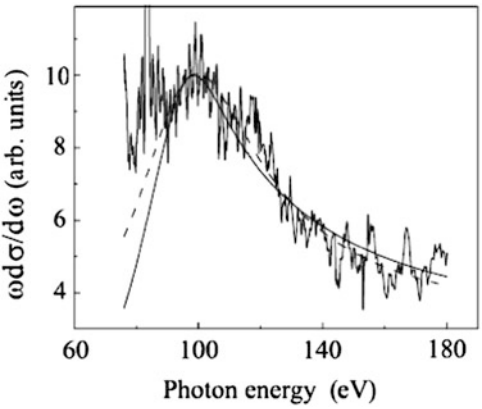


**Fig. 9.8** The spectrum of PBs of an electron with the energy of 0.7 keV on a solid xenon cluster: *"noisy" curve* – experiment, *smooth solid curve* – calculation in view of the dielectric permittivity of an ambient medium, *dashed curve* – calculation in view of the frequency dependence of radiating dipole damping in a medium

The calculations of the cross-section of PBs on xenon atoms and clusters in the work [10] were carried out under the assumption that an atom/cluster is immersed in a gaseous or solid medium with a certain dielectric permittivity that influences the PBs spectrum. As a result, a good conformity between the experimental and calculated data was established.

So experimentally demonstrated in the paper [10] was the important role of PBs of electrons on xenon atoms and clusters in a spectral range corresponding to a giant resonance in photoabsorption, and cooperative effects were recorded that come to reduction of the PBs spectral maximum width with growing number of atoms in a cluster.

## 9.2 Bremsstrahlung on Solid-State Targets

### *9.2.1 PBs of Fast Electrons on Metal Foils*

As was already noted in Chap. 1, one of the first works, in which PBs of fast (relativistic) electrons scattered by a metal foil was reliably recorded, was the paper

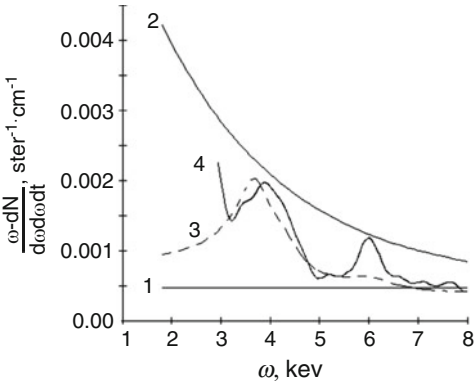


**Fig. 9.9** The spectrum of electrons with an energy of 2.4 MeV scattered in polycrystalline aluminum: *straight line 1* – calculation of ordinary Bs, *curve 2* – calculation of PBs in amorphous aluminum, *curve 3* – calculation of PBs in polycrystalline aluminum, *curve 4* – results of the experiment of [11]

[11]. In this work the measurement of the spectrum of electrons with an energy of 2.4 MeV scattered in a polycrystalline aluminum target was carried out. The position of the spectral maximum of radiation falling on photon energy of 4 keV was exactly recorded (Fig. 9.9).

This maximum, as was predicted in the theoretical work [12], corresponds to the contribution of the polarization channel to total Bs. It corresponds to scattering of a virtual photon to a real photon by the crystallographic plane of target crystallites properly oriented, so that the Bragg condition (Eq. 5.19) is carried out for conversion of a virtual photon to a real photon (see Fig. 5.8). The Eq. 5.19 contains the target reciprocal lattice vector $\mathbf{g}$ that characterizes a crystallographic plane, by which scattering of a virtual photon occurs. It should be noted that the wave vector of a virtual photon forming the eigenfield of a relativistic electron is $|\mathbf{k}|\,\mathbf{v}/v$, where $\mathbf{v}$ is the electron velocity.

The maximum in the spectrum of PBs on a polycrystalline target is characteristic for relativistic electrons. Its central frequency is given by the formula (5.9). It should be noted that in case of nonrelativistic electrons the spectral maximum under consideration degenerates into a "frequency step" according to the formula (5.15).

The calculated curve 3 of Fig. 9.9 corresponds to taking into account three crystallographic planes (111), (220), (222). The spectral maximum at about 6 keV on the experimental curve 4 most probably corresponds to rescattered PBs from crystallographic planes with a high wave vector magnitude.

Further experimental investigation of the absolute cross-section of PBs of relativistic electrons with an energy of 7 MeV scattered by metal foils was carried out in the work [13], in which a source of an electron beam was a microtron. As targets, polycrystalline films of aluminum, copper and nickel were used. The film thicknesses were respectively 8.5 μm (aluminum), 15 μm (copper), 15 μm (nickel). The target was mounted at an angle of 45° to the beam axis, the radiation angle was 90°. Bs was recorded with the use of a Si-Li pin-detector. The angular acceptance of the detector was $1.5 \cdot 10^{-6}$ sterad. The intensity of the electron beam was measured by a Faraday cup placed at the end of the experimental system. The system was not

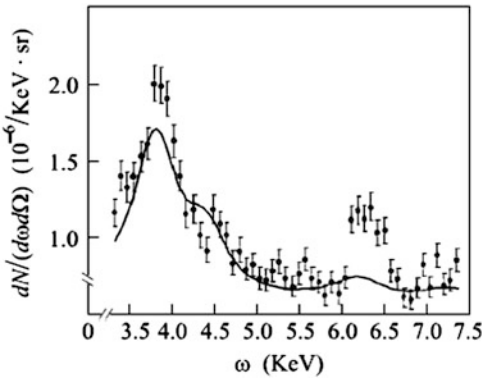


**Fig. 9.10** The spectrum of electrons with an energy of 7 MeV scattered by an aluminum polycrystalline foil: *dots* – experiment, *solid curve* – calculation [13]

separated from the microtron as regards vacuum, inside it a pressure no more than $10^{-5}$ Torr was sustained.

The results of measurements (together with the value of the experimental error) and calculation of the spectrum of PBs of an electron with the energy of 7 MeV on a polycrystalline aluminum target are presented in Fig. 9.10. The experimental and theoretical data of this figure make it possible to separate three maxima in the PBs spectrum, the central energies of which are 3,782 ± 16, 4,560 ± 36, and 6,273 ± 19 eV. In the measured spectrum there is also an ambient background from the microtron that has two sources. The first of them is connected with incoherent PBs and ordinary Bs, its contribution is negligible. The second source is caused by secondary photons appearing as a result of reradiation at the inner walls of the target box and the photon channel. The contribution of this background is 2–4 % of the value of the main maximum in the PBs spectrum presented in Fig. 9.10. In the third spectral maximum there is the contribution of characteristic radiation of photons from the K-line of iron with an energy of 6,403 eV that were produced under the action of scattered electrons of the beam at the inner surface of the target chamber and the photon channel of the system.

Presented in Fig. 9.11 are the results of measurements and calculation of the spectrum of PBs of electrons with the energy of 7 MeV on a nickel target.

The experimental data of Fig. 9.11 are indicative of the presence of three maxima in the spectrum of PBs on a nickel foil, the centers of which have energies of 4,257 ± 15, 5,070 ± 16 and 5,735 ± 11 eV. There is also the contribution of the K-line of iron near a photon energy of 6,400 eV. The spectral maximum at the photon energy of 5,735 eV is of the known instrument origin. It results from ionization of the detector atoms by photons of the K-line of the nickel target since its central energy is exactly equal to the difference of energies of the K-line of nickel (7,475 eV) and silicon atoms (1,740 eV).

Thus in the cited paper the spectra of PBs of relativistic electrons on metal foils were measured and a satisfactory agreement with theoretical predictions for this phenomenon was obtained.

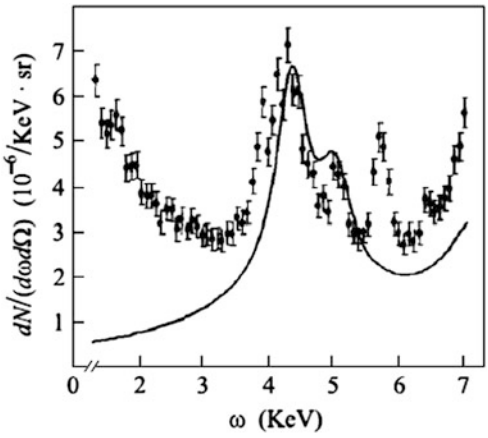


**Fig. 9.11** The spectrum of electrons with an energy of 7 MeV scattered by a nickel foil: *dots* – experiment, *solid curve* – calculation [13]

Bs of nonrelativistic electrons with an energy of 53 keV scattered by gold foils of different thicknesses was studied experimentally and theoretically in the work [14] for four values of photon energy (15, 25, 35, 45 keV) and a radiation angle of 135°. The calculation was carried out with the use of the PENELOPE computer code [15] based on the Monte-Carlo method without considering the polarization channel. The PBs contribution was taken into account within the framework of the stripping approximation [6].

The results of measurements and the theoretical curves obtained in the cited paper are presented in Fig. 9.12 for two values of thickness of a gold foil.

It is seen that for a more thin foil the experimental data are satisfactorily described by the theory of Bs without considering the polarization channel. For a thicker target the experimental dots lie considerably higher than the predictions of the theory of ordinary Bs, however, they unsatisfactorily agree with the theoretical curve describing the PBs contribution within the framework of the stripping approximation.

It should be noted that from the theory of PBs on an atom it is known that the relative contribution of the polarization channel to total Bs decreases with growing energy of a bremsstrahlung photon (see Fig. 2.6). In the experiment of the work [14] the minimum photon energy, for which the measurements were carried out, is 10 keV. This value is represented by a too high quantity, at which the PBs intensity is already rather low. This circumstance is especially essential for nonrelativistic electrons used in the work since the lateral dimension of a virtual photon in this case is not large enough to excite in a coherent manner fluctuations of bound electrons in the target that are the source of PBs. Therefore for recording the contribution of the polarization channel it is preferable to study the low-frequency range of the spectrum of Bs of nonrelativistic electrons with photon energy not exceeding 10 keV.

The results of the paper [14] are also indicate that in the case under consideration a more exact theoretical approach to describe PBs should be used than the approach used in the stripping approximation.

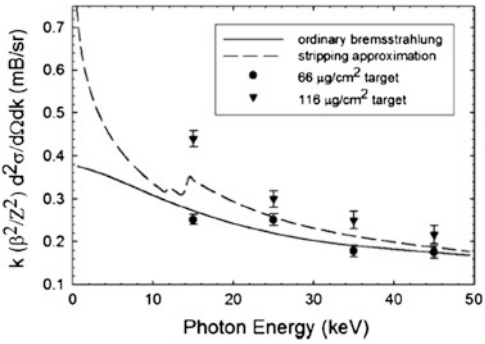


**Fig. 9.12** The experimental and theoretical data on the spectrum of Bs of an electron with the energy of 53 keV scattered by gold films of different thicknesses [14]

### *9.2.2 PBs on Thick Metal Targets Under the Action of β-particles*

In the work [16] bremsstrahlung arising in bombardment of metal targets under the action of β-particles from a $^{204}$Tl radioactive source in a range of photon energies from 5 to 10 keV was investigated experimentally. To measure the spectral distribution of bremsstrahlung photons, the highly sensitive X-PIPS Si (Li) detector with an internal efficiency of 100 % and 97 % for photons with the energy of 5 and 10 keV respectively was used. The resolution of the detector was no less than 190 eV for photon energy of 5.9 keV. To decrease the influence of scattered photons and to restrict the background to a low level, a line of tin fragments and an aluminum foil was used for screening the detector. To obtain correct information on Bs from targets, a special method was used that made it possible to remove the influence of internal Bs and external background. Disks of aluminum (a mass thickness of 293 mg/cm$^2$), titanium (288 mg/cm$^2$), tin (281 mg/cm$^2$), and lead (286 mg/cm$^2$), each 4 cm in diameter, were used as targets.

It should be noted that in contrast to the above works, in which monoenergetic electron beams were used, in the case under consideration the $^{204}$Tl source emits β-particles with energies continuously distributed in a range from 0 to 765 keV.

For comparison with the experiment, several Bs theory versions were used: the Bethe-Heitler theory without considering PBs with a modified Elvert factor for nonrelativistic particles (*EBH*), the Bethe-Heitler theory without considering PBs with a modified Elvert factor for relativistic particles ($F_{\text{mod}}\,BH$), and the Bethe-Heitler theory with a modified Elvert factor for relativistic particles with consideration for PBs ($F_{\text{mod}}\,BH + PB$). In the latter case PBs was calculated in the stripping approximation.

The experimental and theoretical results of the cited work for aluminum and lead targets are given in Figs. 9.13 and 9.14.

As seen from the given figures, the best agreement with experimental data is provided by the Bethe-Heitler theory with a modified Elvert factor for relativistic particles with consideration for the polarization channel (the curves 1 in Figs. 9.13 and 9.14).

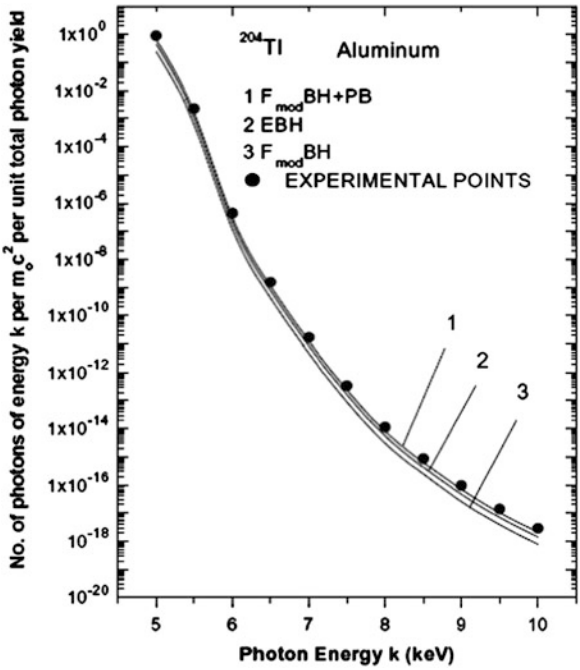


**Fig. 9.13** The plots of the number of Bs photons normalized to the total photon yield as functions of the photon energy for aluminum target [16]

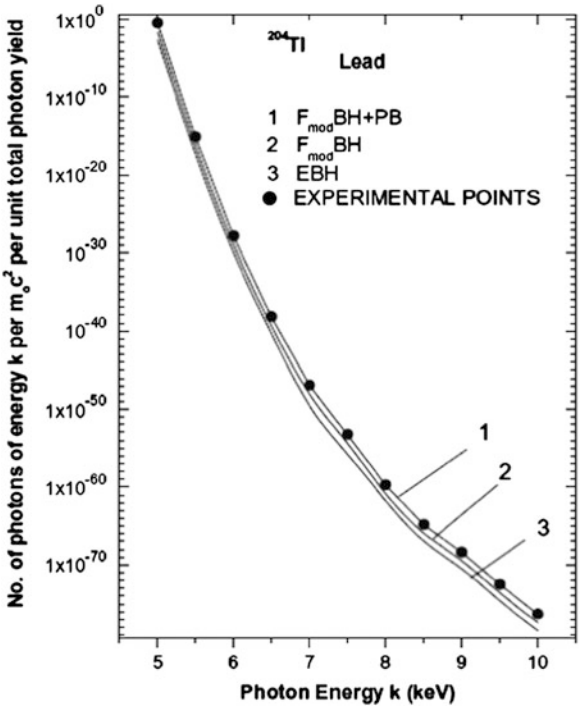


**Fig. 9.14** The plots of the number of Bs photons normalized to the total photon yield as functions of the photon energy for lead target [16]

So the experiment carried out in the work [16] confirms the presence of the appreciable contribution of the polarization channel to total Bs in scattering of β-particles by thick metal targets. The relative value of the polarization contribution to Bs in the considered case is small and is on the average 10 % in a specified spectral range (5–10 keV), decreasing with growing photon energy, especially for targets of elements with a medium and high nuclear charge.

### *9.2.3 Proton Radiation on a Solid-State Target*

In the work [17] the analysis of radiation arising in scattering of protons with energy of several MeV by aluminum target was given that confirmed the important role of PBs in the process under consideration. This analysis was based on the authors' experimental data on Bs of protons and light ions obtained in [18] and the formulas for PBs (called by the authors atomic Bs (AB)) and radiation ionization (RI) derived in the paper [17]. It should be noted that radiation ionization represents simultaneous emission of a photon and ionization of a target in collision with a charged particle. It is characteristic for processes with significant transfer of a momentum in collision.

In the cited work the contributions of different processes to total radiation were discussed. In case of light ions two mechanisms were usually taken into account: bremsstrahlung of secondary electrons (SEB) and Bs of quasi-free electrons (QFEB), the first of which has the boundary frequency $T_m = 2\,m_e\,\mathrm{v}_p^2$, and the second has the boundary frequency $T_r = T_m/4 = m_e\,\mathrm{v}_p^2/2$, where $\mathrm{v}_p$ is the velocity of an incident particle, $m_e$ is the electron mass. Meant by QFEB is radiation of electrons of a target in their scattering in the field of an incident particle. In collision of heavy ions with a target the main role is played by molecular-orbital X-radiation and radiative capture (REC). Nuclear Bs can be neglected in case of fulfilment of the inequation $q\,a << m_T/m_e$ [17], where $q$ is the wave vector transferred from an incident particle to the target, $a$ is the mean atomic radius, $m_T$ is the mass of the target nucleus. This inequation is satisfied in the X-ray range characteristic for physics of atomic collisions.

A new point in comparison with the previous works on radiation of ions on solid-state targets was the fact that the authors in interpretation of their experimental data took into account atomic (polarization) Bs. It was shown in particular that PBs of protons is essential not only in the spectral range near the potential of ionization of a target as was noted in the work [19], but also for high photon energies.

In the experiment [18] self-supporting aluminum foils with a mass thickness of 100 μg/cm$^2$ were used as a target. The thickness of the targets was measured with the use of the Rutherford scattering of protons with the energy of 1 MeV. A beam of incident ions was formed by the Van de Graaff accelerator with a voltage of 5 MV.

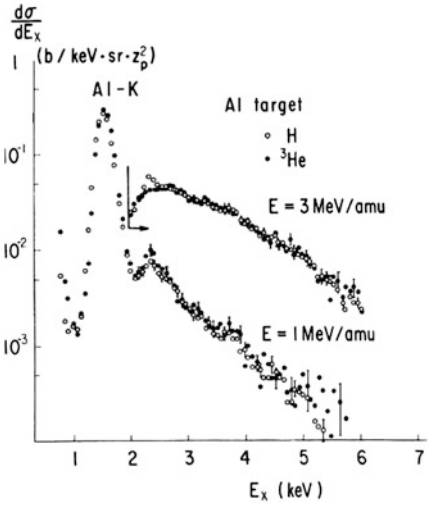


**Fig. 9.15** The spectra of X-radiation in bombardment of aluminum target by protons and $^3$He ions for two energies of incident particles, the detection angle is 90° [18]

The recording of the X-ray spectrum was carried out with the use of a Si-Li detector with a resolution of 205 eV at the photon energy of 6 keV and effective area of 12.5 mm$^2$.

The typical spectra of X-radiation obtained in the work [18] with bombardment of an aluminum target by protons and $^3$He ions with an energy of 1 and 3 MeV per atomic mass unit (1, 3 MeV/amu) are presented in Fig. 9.15. The measurements were carried out for an angle of 90° between the velocity of incident ions and the direction to the photodetector (a detection angle). The angle of incidence of incident particles on the target surface was 45°.

In plotting in Fig. 9.15 the background spectrum was subtracted, but correction taking into account the absorption of X-radiation and the efficiency of the detector was not made. The ordinate was normalized to the squared charge number of an incident particle $Z_p^2$, so from Fig. 9.15 it follows that the measured continuous X-ray spectrum has a scaling with respect to the value $Z_p^2$. Seen in the figure are a maximum caused by characteristic K-radiation of an aluminum atom and a weak peak (at 2.307 keV) connected with the Kα-line of sulfur impurity atoms.

As was already noted, the analysis of the X-ray spectra obtained in the paper [18] was given in the work [17] with the use of the concept of polarization Bs that in the cited work was called atomic. The results of this analysis are given in Figs. 9.16 and 9.17 for two values of energy of protons incident on an aluminum target of 1 and 4 MeV and a detection angle of 90°.

The theoretical curves for PBs and radiating ionization were calculated by the formulas derived in the paper [17], Bs of free electrons was calculated with the use of the expression obtained in the work [20].

Arrowed in Figs. 9.16 and 9.17 are the boundary frequency for Bs of secondary electrons $T_m$ and the boundary frequency for Bs of quasi-free electrons $T_r = T_m/4$.

From the given figures it is seen that in the high-frequency region of the measured spectrum the main channel of radiation is PBs. In case of 1 MeV protons

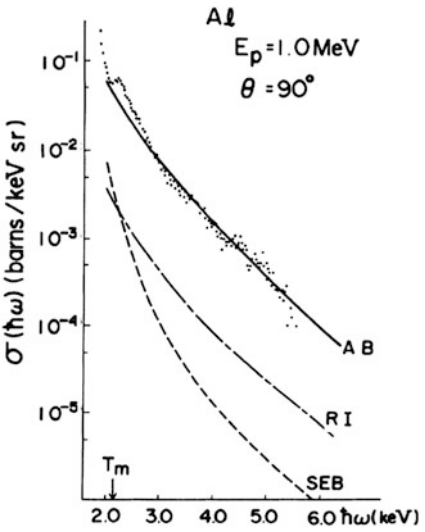


**Fig. 9.16** The comparison of the theory with the experiment for Bs of protons with an energy of 1 MeV bombarding an aluminum target: *solid curve* – PBs (calculation [17]), *dash-and-dot curve* – radiating ionization (calculation [17]), *dashed curve* – radiation of secondary electrons (calculation [20]), *dots* – experiment [18]

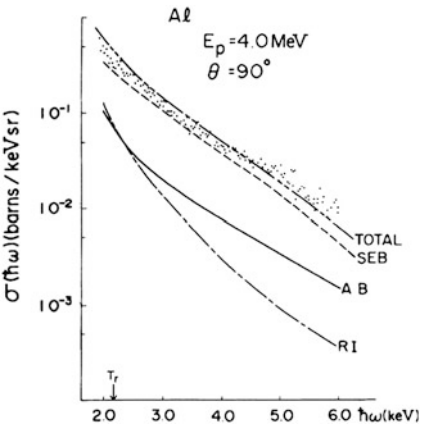


**Fig. 9.17** The same as in Fig. 9.16 for a proton energy of 4 MeV, the *top curve* corresponds to the cross-section of total radiation [17]

this statement is true for $\hbar\omega > T_m$. For 4 MeV protons PBs prevails over other channels of radiation in the range $\hbar\omega > T_r = T_m/4$. In the frequency region $\hbar\omega < T_r$ in this case the cross-section of radiation ionization exceeds the PBs cross-section according to the calculations of the paper [17].

So the analysis of Bs of protons with an energy of 1 and 4 MeV scattered by the aluminum target that was carried out in the paper [17] has shown that among possible mechanisms of radiation PBs prevails in the high-frequency region of the spectrum $\hbar\omega > T_m$. In the range $T_m > \hbar\omega > T_r$ the main contribution is made by Bs of secondary electrons and, finally, in the frequency region $T_r > \hbar\omega$ radiation ionization prevails.

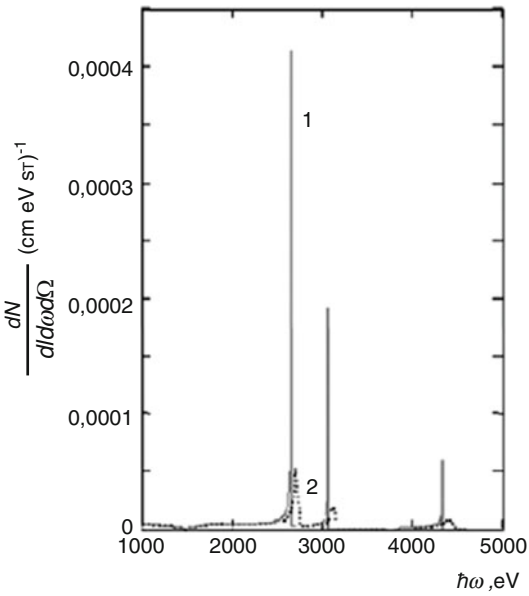


**Fig. 9.18** An abnormal peak in the spectrum of PBs of an electron with an energy of 15 MeV in an aluminum polycrystal: *solid curve* (1) – the radiation angle $\theta = 180°$, *dotted curve* (2) – the radiation angle $\theta = 160°$ (From the paper [21])

### 9.2.4 *Experimental Observation of Coherent Spectral Peaks of PBs of Relativistic Electrons in a Polycrystal in Backward Radiation*

Theoretically predicted in the work [21] was a sharp increase of the intensity of PBs of a relativistic electron scattered in a polycrystal, when the angle θ between the wave vector of a bremsstrahlung photon and the electron velocity is 180° (backward radiation). The results of calculations of the PBs spectra carried out in the cited work are presented in Fig. 9.18 for an electron with the energy of 15 MeV scattered in an aluminum polycrystal for two radiation angles.

Three spectral maxima on the curves of Fig. 9.18 correspond to coherent PBs with transfer of the wave vector excess to different reciprocal lattice wave vectors (see the formula (5.15)).

In the work [21] the following expression was derived that describes the intensity of PBs of a relativistic electron in a polycrystal in the region of the spectral maximum as a function of the radiation angle and the electron velocity:

$$\Phi_{\max}(\theta,\, \gamma_*) \approx \frac{2\,\gamma_*\, \sin(\theta/2)}{\sqrt{\cos^2(\theta/2) - \cos\theta/\left(4\,\gamma_*^2\right)}}, \tag{9.4}$$

where $\gamma_*$ is the Lorenz factor in a medium that takes into account the change of the phase velocity of radiation in a substance. From the formula (9.4) it follows that the value of a spectral peak for radiation angles far from 180° is proportional to the

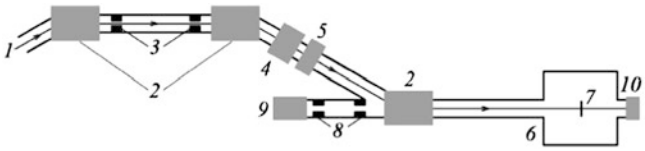


**Fig. 9.19** The diagram of the modified "Roentgen" experimental system: *1* – vacuum channel for an electron beam; *2* – rotary magnets; *3, 8* – collimators; *4* – quadrupole lenses; *5* – beam corrector; *6* – vacuum chamber; *7* – target; *9* – X-ray detector; *10* – beam proportional chamber [22]

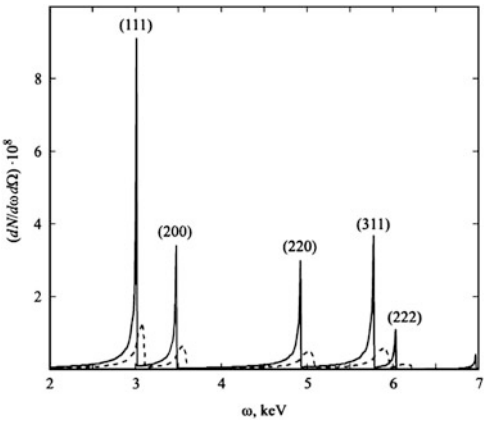


**Fig. 9.20** The calculated spectrum of coherent PBs of a relativistic electron scattered by a copper polycrystal for two radiation angles: *solid curve* – $\theta = 180°$, *dashed curve* – $\theta = 160°$ (From the paper [22])

relativistic factor $\gamma_*$; and if $\theta = 180°$, then $\Phi_{max} \sim \gamma_*^2$, which in the limit $\gamma_* >> 1$ means a sharp increase of the PBs intensity.

In the paper [22] the experimental confirmation of the theoretical conclusions of the work [21] was obtained. The measurements of the spectra of PBs of electrons with an energy of 7 MeV scattered in a polycrystalline copper target were carried out for backward radiation. The basic diagram of the experimental system is given in Fig. 9.19.

Backward PBs was recorded by the PIN detector 9, the energy resolution of which was 152 eV. Serving as the target 7 was a foil of electrical copper with a thickness of 25 μm.

The results of calculation of the spectrum of coherent PBs of a relativistic electron in a copper polycrystal for the above problem parameters are presented in Fig. 9.20.

From the given figure it is seen that with the radiation angle approaching 180° the intensity of coherent PBs at the maximum of the frequency dependences sharply increases, and the width of a spectral peak decreases. Three numbers in the parentheses above spectral peaks number a crystallographic plane, by which a virtual photon of the electron eigenfield is scattered to a real Bs photon (see Fig. 5.8).

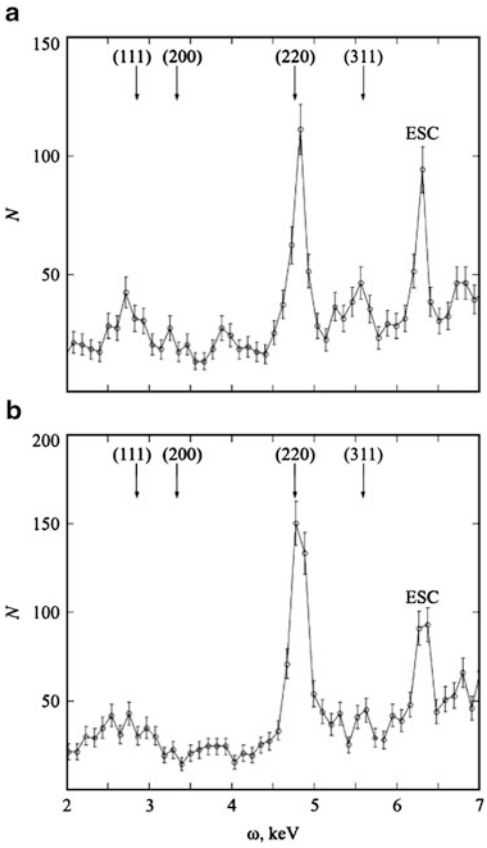


**Fig. 9.21** The experimental spectra of PBs of a relativistic electron scattered by a copper foil in backward radiation: (**a**) normal orientation of the sample plane with respect to an electron beam, (**b**) random orientation of the target plane with respect to an electron beam, (**c**) another random orientation of the target (From the work [22])

It should be noted that the spectrum of coherent PBs presented in Fig. 9.20 corresponds to averaging over orientations of crystallites forming the polycrystal under the assumption of their isotropic distribution. This fact is expressed by the formula (5.14), in which the integral with respect to the normalized solid angle of the reciprocal lattice vector $d\Omega_{\mathbf{g}}/4\pi$ describes this averaging. In case of a texture crystal, when the isotropism of the distribution of the reciprocal lattice vectors $\mathbf{g}$ is violated, the polycrystal becomes partially oriented, it is necessary to introduce into the integral on the right side of the Eq. 5.14 the distribution function $f(\mathbf{g})$ reflecting a concrete texture of a polycrystal. A texture can appear in a polycrystalline sample such as a thin foil in the process of its manufacturing or by other reasons.

To investigate the microstructure of a target, in the work [22] the measurements of the spectra of coherent PBs were carried out for different orientations of a sample of a copper foil with respect to an electron beam. The results of these experiments are presented in Fig. 9.21a–c).

The comparison of the PBs spectra (Fig. 9.21) measured for a real target with the calculated spectrum (Fig. 9.20) obtained for a polycrystalline target (without texture) shows a change of the PBs photon yield (reflection) caused by different

crystallographic planes. For example, in Fig. 9.21a the (111) reflection yield is strongly suppressed in comparison with the theoretical data for an isotropic polycrystal and the (200) reflection yield is practically absent. At the same time from Fig. 9.21b it follows that at a specified orientation of a target with respect to an electron beam an increase of the (220) reflection yield is observed with other reflections suppressed. The PBs spectrum shown in Fig. 9.21c, corresponding to another abnormal orientation of a target, has another form differing from the spectra of Fig. 9.21a, b.

The comparison of reflection yields was made on the basis of comparison of the values of spectral maxima of PBs with the "instrument" spectral maximum at photon energy of 6.3 keV that in Fig. 9.21 is designated by the symbol ESC. The position of this spectral maximum is defined by the difference of the energy of a photon of the K-line of characteristic copper radiation and the energy of the silicon photoabsorption edge in the X-ray detector. It is seen that the spectral width of the "instrument" peak is comparable with the widths of peaks of coherent PBs of a relativistic electron with a specified energy (7 MeV) in backward radiation. Based on this fact, the authors of the paper [22] made an assumption that the real spectral width of PBs peaks in backward radiation is close to the spectral width of characteristic radiation of the copper K-line, which requires additional measurements of peaks under study by a detector with higher energy resolution.

It should be noted that according to the theoretical analysis carried out in the work [21], the spectral width for coherent PBs in backward radiation decreases in inverse proportion to the squared energy of an incident electron (with neglected saturation effect that is caused by changing phase velocity of radiation in a medium). For radiation angles less than 180° narrowing of the line of coherent PBs in a polycrystal is inversely proportional to the electron energy in the first degree.

Thus it can be concluded that narrow spectral maxima of coherent PBs recorded in the cited work were found to be rather sensitive to the structure of a polycrystalline target, which is of interest for development of a new energy dispersion method for substance structure diagnostics with the use of recording PBs spectra [23].

## References

1. Verkhovtseva, E.T., Gnatchenko, E.V., Pogrebnjak, P.S.: Investigation of the connection between giant resonances and atomic bremsstrahlung. J. Phys. B At. Mol. Phys. **16**, L613 (1983)
2. Haensel, R., Keitel, G., Schreiber, P., Kunz, C.: Optical absorption of solid krypton and xenon in the far ultraviolet. Phys. Rev. **188**, 1375 (1969)
3. Amusia, M.Y., Zimkina, T.M., Kuchiev, M.Y.: Wide emission bands in radiation of atoms under influence of rapid electrons. Zh. Tekh. Fiz. **52**, 1424 (1982) (in Russian)
4. Verkhovtseva, E.T., Gnatchenko, E.V., Zon, B.A., Nekipelov, A.A., Tkachenko, A.A.: Bremsstrahlung in electron scattering by xenon. Zh. Eksp. Teor. Fiz. **98**, 797 (1990)
5. Portillo, S., Quarles, C.A.: Absolute doubly differential cross sections for electron bremsstrahlung from rare gas atoms at 28 and 50 keV. Phys. Rev. Lett. **91**, 173201 (2003)

6. Korol, A.V., Lyalin, A.G., Solovy'ov, A.V., Avdonina, N.B., Pratt, R.H.: On the stripping approximation in the bremsstrahlung process. J. Phys. B **35**, 1197 (2002)
7. Buimistrov, V.M., Trakhtenberg, L.I.: The role of atomic electrons in bremsstrahlung. Sov. Phys. JETP **46**, 447 (1977)
8. Kissel, L., Quarles, C.A., Pratt, R.H.: Shape functions for atomic-field bremsstrahlung from electrons of kinetic energy 1–500 keV on selected neutral atoms $1 \leq Z \leq 92$. At. Data Nucl. Data Tables **28**, 381 (1983)
9. Astapenko, V.A.: Bremsstrahlung of fast charged particles on clusters in a wide spectral range. JETP **101**, 3 (2005)
10. Gnatchenko, E.V., Nechay, A.N., Samovarov, V.N., Tkachenko, A.A.: Polarization bremsstrahlung from xenon atoms and clusters: a cooperative effect contribution. Phys. Rev. A **82**, 012702 (2010)
11. Blashevich, S., Chepurnov, A., Grishin, V., et al.: Polarization bremsstrahlung of relativistic electrons in aluminium. Phys. Lett. A **254**, 230 (1999)
12. Nasonov, N.N.: Collective effects in the polarization bremsstrahlung of relativistic electrons in condensed media. NIM B **145**, 19 (1998)
13. Astapenko, V.A., Kubankin, A.S., Nasonov, N.N., et al.: Measurement of the polarization bremsstrahlung of relativistic electrons in polycrystalline targets. JETP Lett. **84**, 281 (2006)
14. Williams, S., Quarles, C.A.: 1Absolute bremsstrahlung yields at 135° from 53-keV electrons on gold film targets. Phys. Rev. A **78**, 062704 (2008)
15. Salvat, F., Fernandez-Varea, J.M., Sempau, J., Llovet, X.: Monte Carlo simulation of bremsstrahlung emission by electrons. Radiat. Phys. Chem. **75**, 1201 (2006)
16. Singh, T., Kahlon, K.S., Dhaliwal, A.S.: Total bremsstrahlung spectral photon distributions in metallic targets in the photon energy range of 5–10 keV by 204Tl beta particles. NIM B **267**, 737 (2009)
17. Ishii, K., Morita, S.: Continuum x rays produced by light-ion-atom collisions. Phys. Rev. A **30**, 2278 (1984)
18. Ishii, K., Morita, S., Tawara, H.: Bremsstrahlung induced by proton and 3He-ion bombardments in the 1-4-MeV/amu energy range. Phys. Rev. A **13**, 131 (1976)
19. Amusia, M.Y.: "Atomic" bremsstrahlung spectrum. Comments At. Mol. Phys. **11**, 123 (1982)
20. Yamadera, A., Ishii, K., Sera, K., et al.: Quasifree-electron bremsstrahlung induced by the projectile field. Phys. Rev. A **23**, 24 (1981)
21. Astapenko, V., Nasonov, N., Zhukova, P.: Anomalous peak in the spectrum of polarizational bremsstrahlung from relativistic electrons moving through a solid target. J. Phys. B **40**, 1337 (2007)
22. Alekseev, V.I., Vokhmyanina, K.A., Eliseev, A.N., et al.: Measuring coherent peaks of polarization bremsstrahlung from relativistic electrons in polycrystalline targets in backscattering geometry. Tech. Phys. Lett. **38**, 294 (2012)
23. Astapenko, V.A., Gostishchev, N.A., Zhukova, P.N., et al.: Modification of the EDXD method for diagnostics of polycrystalline and fine-grained media. Bull. Russ. Acad. Sci. Phys. **76**, 863 (2008)